Prestack depth migration for complex 2D structure using phase-screen propagators

Peter Roberts, Lian-Jie Huang, Los Alamos National Laboratory, Charles Burch, Conoco Inc., Michael Fehler and Steven Hildebrand, Los Alamos National Laboratory.*

Summary

We present results for the phase-screen propagator method applied to prestack depth migration of the Marmousi synthetic data set. The data were migrated as individual common-shot records and the resulting partial images were superposed to obtain the final complete image. Tests were performed to determine the minimum number of frequency components required to achieve the best quality image and this in turn provided estimates of the minimum computing time. Running on a single processor SUN SPARC Ultra 1, high quality images were obtained in as little as 8.7 CPU hours and adequate images were obtained in as little as 4.4 CPU hours. Different methods were tested for choosing the reference velocity used for the background phase-shift operation and for defining the slowness perturbation screens. Although the depths of some of the steeply dipping, high-contrast features were shifted slightly, the overall image quality was fairly insensitive to the choice of the reference velocity. Our tests show the phase-screen method to be a reliable and fast algorithm for imaging complex geologic structures, at least for complex 2D synthetic data where the velocity model is known.

Introduction

Exploration geophysicists continue searching for fast, accurate seismic imaging algorithms that can be used for migrating large 3-dimensional survey data collected in geologically complex regions. Methods are sought that can provide the image accuracy that existing approaches such as finite-difference are capable of producing, but that can process the large volumes of data in a fraction of the time. To this end, we have been testing a Fourier migration method, known alternatively as either the phase-screen (Huang & Wu, 1996) or split-step Fourier (Stoffa et al., 1990) method, on increasingly more complex model data. The eventual goal is to determine the method's usefulness for 3D prestack depth migration of large seismic surveys conducted over complex oil bearing formations such as subsalt and overthrust structures.

As an intermediate goal, the phase-screen method was tested on prestack depth migration of the well-known 2D Marmousi data, which are synthetic common-shot gathers generated by the Institut Français du Pétrole (IFP) for a model derived from the geologic structure of the Cuanza Basin in Angola (Bourgeois et al., 1991). The Marmousi data have received considerable attention as an "acid test" for seismic imaging and velocity estimation techniques (Versteeg, 1994). Virtually all popular migration methods have been tested on the Marmousi data and significant differences are observed in the image quality obtained. Some examples of the best published images were obtained using methods such as finite-difference (Bevc, 1997), common-offset split-step DSR (Popovici, 1996), and semi-recursive Kirchoff (Bevc, 1997).

Figure 1 shows a grayscale plot of the Marmousi velocity model. Most migration methods do well at imaging the shallower features of the thrust sheet and listric faults. The most difficult areas to image accurately are the anticlinal features under the thrust sheet and under the high-velocity salt wedges at the bottom of the model. Perhaps the most critical part of the model to image, in terms of petroleum prospects, is the low-velocity lens centered at about 6500 m horizontal position and 2500 m depth, near the top of the deeper anticlinal feature.

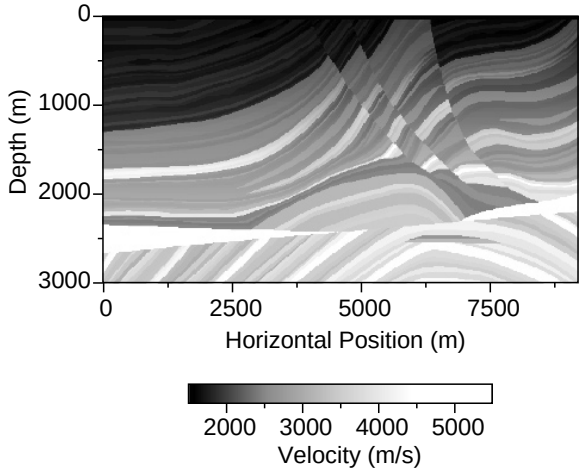

Fig. 1 Marmousi velocity model used to test the accuracy of the phase-screen method for imaging complex structures.

We present here a brief description of the phase-screen method and how it was used for prestack depth migration of common-shot data. We then show images of the best phase-screen migration results obtained for the Marmousi data using different frequency bandwidths. Finally we discuss different methods for specifying the background reference velocity used, and their effects on the accuracy of the Marmousi migrated image.

The phase-screen method

Phase-screen propagators have been in use for some time to model one-way forward wave propagation in laterally heterogeneous media. The algorithm for back propagation of zero-offset reflection data was presented by Stoffa et al. (1990) and given the name "split-step Fourier" method. It is similar in many ways to the phase-shift-plus-interpolation (PSPI) method of Gazdag & Sguazzero (1984) except that the intermediate step of interpolating multiple downward continued depth slices is replaced by a single interaction with a slowness perturbation screen in the spatial domain at each depth.

The surface wavefield $P(x,z=0,t)$ is first Fourier transformed over t. Then the downward continued wavefield at each depth step $P(x,z+\Delta z)$, for each frequency component ω, is obtained from the previous depth step using:

(1)

$$P(x,z+\Delta z) = \exp\left[\pm i\omega\left(\frac{1}{v(x,z)} - \frac{1}{v_0(z)}\right)\Delta z\right] \bullet \mathrm{IFFT}_{k_x}^{(*)}\left\{\exp\left[\pm i k_z \Delta z\right] \bullet \mathrm{FFT}_x^{(*)}\left\{P(x,z)\right\}\right\},$$

where:

$$k_z = \sqrt{\frac{\omega^2}{v_0^2(z)} - k_x^2}\,.$$

The phase-screen term is the first complex exponential on the right side of the equation. The second exponential is the background phase-shift term for laterally homogeneous media. For prestack migration both source and receiver fields, P_S and P_R, are propagated downward simultaneously using the formula above, where the sign of the exponents in the screen and phase-shift terms are taken positive for forward propagation of the source and negative for backward propagation of the receiver field. Also, the complex conjugate of the two Fourier transforms is used for the receiver field. Because source and receivers are propagated simultaneously, the imaging condition at each image point (x,z) for a given shot record, n, may be written:

(2) $$I_n(x,z) = \sum_{\omega} -i\omega P_{S_n}^*(x,z,\omega) \bullet P_{R_n}(x,z,\omega).$$

For the Marmousi data, each shot-record was migrated separately and the resulting partial images were summed to obtain the final complete image. This allowed us to use different reference velocities, $v_0(z)$, for each shot-record so that the velocity perturbations could be kept to a minimum in different parts of the model. Thus, the final complete image is obtained by summing the partial images for all shot records:

(3) $$I_{\text{total}}(x,z) = \sum_n I_n(x,z).$$

In general, phase-shift migration methods are computationally efficient because of the heavy use of fast Fourier transforms, the avoidance of convolution integrals, and the ability to reduce the number of frequency components to be migrated. These features make FFT methods particularly useful for sequential common-shot migration because the computational overhead of processing one shot record at a time is small and large multiple-shot data sets can be broken down into small independent partial migrations that can run on a single processor. This, in turn, makes it easy to parallelize phase-shift algorithms by farming out individual shot records to multiple processing elements (e.g., Roberts et al., 1996).

Marmousi data migration

The Marmousi velocity model (Fig. 1) has maximum physical dimensions of x = 9200 m and z = 3000 m. The model is gridded with nx = 369 and nz = 751 grid points. The Marmousi data set consists of 240 common-shot records with 96 receiver traces each, and 726 samples/trace. Shot and receiver spacings are both 25 m with a minimum offset of 200 m. The trace sampling interval is 4 ms. To take full advantage of the FFT's efficiency in the phase-screen migration, all appropriate data and model dimensions were padded to the next power of 2. Because we only perform spatial FFT's on the x dimension, the resulting migration image area was 512 by 751 in size. For the initial time-domain FFT's, each trace was zero-padded to 1024 samples. The wavelet used for the forward source propagation was derived from the first reflected arrival on a receiver trace recorded over the flat-layered portion of the model. The maximum spectral bandwidth of the data is approximately 10 - 50 Hz and is peaked sharply at about 25 Hz. Thus, it is not necessary to migrate frequencies outside of this band.

After the initial time-domain FFT, the selected frequency components for the source and each trace of the current shot record are stored in their proper x locations in the two propagation arrays, P_S and P_R, respectively. The remaining portions of these 512-element arrays are set to zero and an x-taper is applied to the ends of the live frequency-domain data. After choosing an appropriate reference velocity, the background phase-shift operators and the phase-screens are calculated for each depth step in the velocity model and Equation (1) is used recursively to propagate the source and receiver fields downward, one

frequency at a time. At each depth step, the imaging condition is applied to the current frequency component and the result is added into the sum in Equation (2). Each successive shot-record is processed in the same manner and the partial images are added into the cumulative summation in Equation (3). For the tests reported here, the phase-screen code was run serially on a single-processor workstation with shot records processed sequentially.

Results

Migration tests were performed mainly to determine the maximum accuracy and processing efficiency obtainable with the phase-screen method. The two adjustable parameters we felt were most important to test first are the migration frequency band and the background reference velocity. The frequency band and actual number of frequencies used will affect both the accuracy and computing speed, whereas the choice of reference velocity will affect only the accuracy.

The best image obtained so far is shown in Figure 2. This image was produced using 80 frequency components from 10 to 50 Hz. A different reference velocity was used for each shot record as follows. At each depth in the velocity model we averaged the velocities over all horizontal positions within each shot record's physical bounds, i.e., between the shot location itself and the location of the furthest receiver for that shot. This allows the reference velocity to vary across different regions of the model and helps to keep the maximum velocity perturbations within the range of applicability for phase-screen migration.

As shown clearly in Figure 2, the phase-screen method produces a highly detailed and accurate migrated image of the Marmousi data. The deep anticlinal features in the target prospect zone beneath the salt wedges are imaged particularly well. This specific run with 80 frequencies completed in 17.4 CPU hours on a single-processor SUN SPARC Ultra 1 workstation.

Figures 3 and 4 show the effects of reducing the number of frequency components used in the migration. The frequency band was successively halved until the image started losing significant detail. Figure 3 shows the image obtained for 40 frequencies from 15 to 35 Hz. This image retains all of the most important structural details seen in Figure 2, but the migration completed in 8.7 CPU hours. In Figure 4, only 20 frequencies from 20 to 30 Hz were used and the run completed in 4.4 CPU hours. The general structure and the anticlinal target zone are still imaged well enough to identify the major features, but the limited bandwidth does not provide enough resolution to discern some of the finer layering. We feel this image is nearing the limit of what might be considered adequate for production prospecting.

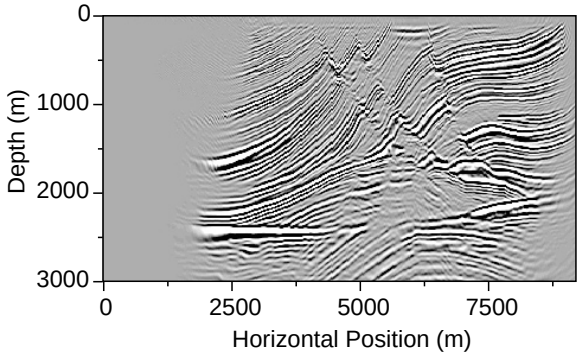

Fig. 2 Image obtained by common-shot prestack depth migration of the IFP Marmousi synthetic data set using the phase-screen method. Frequency components from 10 to 50 Hz were used in the migration.

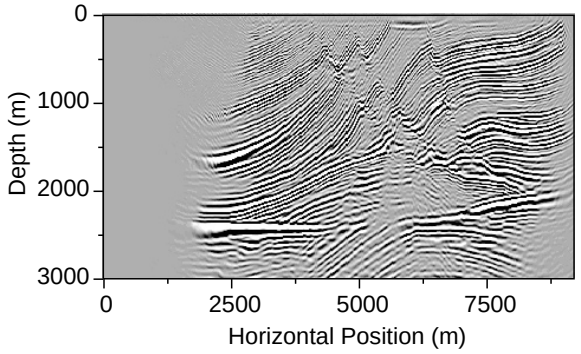

Fig. 3 Same as Fig. 2, except frequency range used in migration is 15 to 35 Hz.

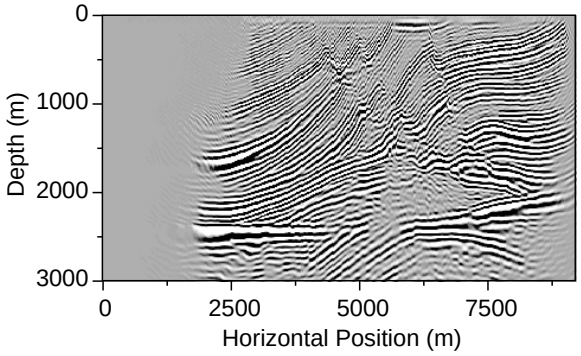

Fig. 4 Same as Fig. 2, except frequency range used in migration is 20 to 30 Hz.

The tests we performed on adjusting the reference velocity showed surprisingly little difference in the image quality. Narrowing the width of the averaging region under each shot record by 1/2 had no discernible effect at all. The largest discrepancies relative to the image in Figure 2 were observed when we averaged the entire model over all horizontal positions at each depth and used this single average profile as the reference velocity for every shot record. In this case, the deep anticlinal target remained unchanged, but significant errors were observed in the locations of some of the high-contrast, steeply dipping events associated with the thrust sheet and listric faults.

Discussion

The phase-screen method has been in use in other scientific disciplines for some time, but only recently was introduced in the seismic exploration community as primarily a poststack method for small velocity perturbations (Stoffa et al., 1990). It has since been extended to allow multiple reference velocities within single shot records (Kessinger, 1992) and has been successfully tested on common-offset DSR migration of the Marmousi data (Popovici, 1996). We have applied the phase-screen method directly to the common-shot Marmousi data and demonstrated that it works extremely well for prestack migration without the need for re-sorting traces. Because the phase-screen propagator is used to downward continue both the source and receiver fields simultaneously, the prestack imaging condition is easily satisfied by frequency-domain summation, without the need for computing travel times from the source to each image point.

Based on the Marmousi tests presented here, we believe the accuracy and robustness of the phase-screen migration method have been confirmed for complex, synthetic 2D data. The vast majority of migrated events in Figure 2 correspond to actual horizons in the Marmousi velocity model, and the imaging accuracy is reasonably insensitive to the choice of frequency band and reference velocity. As mentioned, though, significant errors were observed in the shallower high-contrast reflectors when a single model-averaged reference velocity was used for all shot records. In general these shallow events were deeper in the single-reference-velocity image than in the multiple-reference-velocity image. These errors were not propagated down into the deeper parts of the image, however. We believe this may be due in part to cancellation of shallow-region positive errors by approximately equal magnitude negative errors in the deeper regions. The target anticline region itself is not as complex as the thrust region above it and, thus, is imaged correctly because the cumulative phase errors are small when the migrated data reach the target depth.

Our next goals are to test the same code on a real 2D seismic field survey and then implement a parallel 3D version. Because common-shot migration can be easily parallelized across shot records, and the memory and computation requirements for phase-screen migration are not prohibitive, a simple message-passing parallel computing model can be used. This has been shown to be an effective approach to parallel 3D migration for the PSPI algorithm (Roberts et al., 1996).

Conclusion

We tested the phase-screen method for common-shot prestack depth migration of the Marmousi data set. The method produced an accurate and robust image of the Marmousi velocity model in approximately 9 CPU hours on a single-processor SUN SPARC Ultra 1 workstation. An adequate, but less accurate, image was obtained in about 4 CPU hours by reducing the number of frequency components migrated. Because the method is reasonably insensitive to the choice of reference velocities, it should perform well on real data and the code can be easily parallelized for processing large 3D seismic surveys.

Acknowledgments

This work is part of the Advanced Computational Technology Initiative. Funding came from the Department of Energy Office of Basic Energy Sciences through contract W-7405-ENG-36. Additional cost-shared support came from our numerous project collaborators in the oil and gas industry.

References

Bevc, D., 1997, Imaging complex structures with semi-recursive Kirchoff migration, Geophysics, **62**, 577-588.

Bourgeois, A., Bourget, M., Lailly, P., Poulet, M., Ricarte, P., and Versteeg, R., 1991, Marmousi, model and data: Proc. 1990 EAEG workshop on Practical Aspects of Seismic Data Inversion.

Gazdag, J., and Sguazzero, P., 1984, Migration of seismic data by phase shift plus interpolation: Geophysics, **49**, 124-131.

Huang, L.-J., and Wu, R.-S., 1996, Prestack depth migration with acoustic screen propagators: 66th Ann. Internat. Mtg., Soc. Expl. Geophys., Expanded Abstracts, 415-418.

Kessinger, W., 1992, Extended split-step Fourier migration: 62nd Ann. Internat. Mtg., Soc. Expl. Geophys., Expanded Abstracts, 684-687.

Popovici, A.M., 1996, Prestack migration by split-step DSR: Geophysics, **61**, 1412-1416.

Roberts, P.M., Alde, D.M., House, L.S., Higginbotham, J.H., and Sukup, D.V, 1996, Fast 3-D prestack depth migration with a parallel PSPI algorithm: 66th Ann. Internat. Mtg., Soc. Expl. Geophys., Expanded Abstracts, 1021-1024.

Stoffa, P.L., Fokkema, J.T., de Luna Freire, R.M., and Kessinger, W.P., 1990, Split-step Fourier migration: Geophysics, **55**, 410-421.

Versteeg, R., 1994, The Marmousi experience: Velocity model determination on a synthetic complex data set, The Leading Edge, **13**, 927-936.